

Protective strategy for the caudate lobe bile duct during left hemihepatectomy based on imaging data analysis

Zhengyi Wu^{1,*}, Liang Sun^{1,*}, Ke Ning^{2,*}, Zhendong Chen¹, Zhipeng Wu¹, Hanqing Yang¹, Jinlong Yan¹, Xiangbao Yin¹

¹Department of General Surgery, Second Affiliated Hospital of Nanchang University, Nanchang, China

²Department of Emergency, First Affiliated Hospital of Nanchang University, Nanchang, China

Purpose: This study was performed to analyze the rule of confluence of the caudate lobe bile duct (CLD) into the left hepatic duct (LHD) and to discuss the protective strategy during left hemihepatectomy.

Methods: MRI of 400 patients and T-tube angiography images of 100 patients were collected, and the imaging rules of the confluence of the CLD into the LHD were summarized. The clinical data of 33 patients who underwent left hemihepatectomy using the protective strategy were analyzed.

Results: MRI and T-tube angiography images showed that the length from the confluence point of the CLD into the LHD to the confluence of the left and right hepatic ducts was 1.19 ± 0.40 cm and 1.26 ± 0.39 cm, respectively. The average angle between the longitudinal axis of the 2 bile ducts was $68.27^\circ \pm 22.59^\circ$ and $66.58 \pm 22.88^\circ$, respectively. Coronal and cross-sectional images showed that inflow from the foot side to the cranial side was noted in 79.8% and 82.0% of patients, respectively, and inflow from the dorsal to the ventral side was observed in 84.5% and 88.0%, respectively. Based on these imaging rules, the safe transection length and plane were summarized, and the CLD was effectively protected in 33 cases of left hemihepatectomy.

Conclusion: In left hemihepatectomy, the LHD should be transected at least 1.5 cm away from the confluence of the left and right hepatic ducts, and the plane of transection should be oblique to the dorsal side at an angle of 45° with the LHD, these parameters represent an effective strategy to protect the CLD.

[Ann Surg Treat Res 2023;105(6):369-375]

Key Words: Caudate lobe, Hepatectomy, Hepatic duct, Imaging

INTRODUCTION

Left hemihepatectomy is one of the classical surgical procedures to treat bile duct stones and benign and malignant tumors in the left lobe of the liver clinically [1]. When left hemihepatectomy is performed to cut off the left hepatic duct

(LHD), the caudate lobe bile duct (CLD) that drains into the LHD is easily damaged or directly transected, and the CLD can cause a series of complications of bile duct injury, such as bile duct stenosis or atresia. These complications increase the chance of CLD stone formation, which may further progress to cause atrophy, fibrosis, and even carcinogenesis of the liver

Received July 27, 2023, Revised September 18, 2023, Accepted October 6, 2023

Corresponding Author: Xiangbao Yin

Department of General Surgery, Second Affiliated Hospital of Nanchang University, No. 1, Minde Road, Nanchang 330006, China.

Tel: +86-791-86259631, **Fax:** +86-791-86259631, **E-mail:** yxbefy@126.com, **ORCID:** https://orcid.org/0009-0007-3398-0040

Co-Corresponding Author: Jinlong Yan

Department of General Surgery, Second Affiliated Hospital of Nanchang University, No. 1, Minde Road, Nanchang 330006, China.

Tel: +86-791-86311529, **E-mail:** yjl19880608@126.com, **ORCID:** https://orcid.org/0000-0001-6234-6224

*Zhengyi Wu, Liang Sun, and Ke Ning contributed equally to this study as co-first authors.

Copyright © 2023, the Korean Surgical Society

© Annals of Surgical Treatment and Research is an Open Access Journal. All articles are distributed under the terms of the Creative Commons Attribution Non-Commercial License (<http://creativecommons.org/licenses/by-nc/4.0/>) which permits unrestricted non-commercial use, distribution, and reproduction in any medium, provided the original work is properly cited.

tissue [2,3]. One of the author's patients with hepatobiliary stone disease underwent left hepatectomy after the first illness, and the hyperplasia and hypertrophy of the caudate lobe provided a compensatory function after the operation so that right hepatectomy was available after the second illness. There have been several studies of right and left hepatectomy with caudate lobe preservation alone, all of which have shown the importance of protecting caudate lobe function [4,5]. Protecting the CLD is the most important part of protecting the caudate lobe in the left hemihepatectomy.

At present, many relevant studies at home and abroad focus on exploring the resection modality of the caudate lobe. Reports about protecting the CLD during left hemihepatectomy are limited, and effective strategy to protect the CLD is not currently available. Imaging data were analyzed to summarize the rule that the CLD converges into the LHD, providing the possibility of bile duct protection by the caudate lobe. We conducted this study precisely based on this rule.

In this study, the MRI data of 400 patients in our unit and the T-tubulogram data of 100 patients were retrospectively analyzed to summarize the imaging rules of the CLD entering the LHD, to provide a basis for a protection strategy of the CLD intraoperatively, and to verify the efficacy and safety of this strategy in 33 left hemihepatectomies in the Second Affiliated Hospital of Nanchang University.

METHODS

This study was approved by the Medical Research Ethics Committee of the Second Affiliated Hospital of Nanchang University (No. 2020-123).

General imaging information

Data from hepatobiliary pancreatic MRI of hepatobiliary patients and T-tube cholangiography images of patients after bile duct exploration in the authors' unit between January 2018 and December 2021 were collected. The inclusion criteria were as follows: the CLD was clear on imaging data, and the data could be measured. Exclusion criteria: data from CLD that were indistinct on visualization of bile ducts were excluded; patients under the age of 18 years. MRI data of 400 patients (200 patients of both sexes) and T-tube cholangiography images of 100 patients (50 patients of both sexes) were finally collected.

Imaging examination

Magnetic resonance imaging

The MRIs of 400 patients were obtained by GE 3.0T MRI scanning (General Electric Healthcare) in the Second Affiliated Hospital of Nanchang University. Specifically, MRI hydrographic imaging sequence and two-dimensional/three-dimensional

magnetic resonance cholangiopancreatography image data were analyzed.

T-tube cholangiography

First, mix meglumine diatrizoate with normal saline at a 1:1 ratio. Second, draw an appropriate amount of contrast agent, and slowly inject it into the T-tube. Perform multiposition fluoroscopy and collect images. Third, analyzed the image data from the T-tube cholangiography.

Imaging observation index

The following measurements were obtained using MRI and T-tube cholangiography imaging data. First, the length from the confluence point of the CLD into the LHD to the confluence of the left and right hepatic ducts; the angle between the longitudinal axis of the CLD entering the LHD and the longitudinal axis of the initial segment of the LHD (Fig. 1). Second, coronal plane and cross-section in the direction of the CLD flowing into the LHD (Fig. 2).

Clinical data

Based on the imaging rules of the confluence of the CLD into the LHD, we adopted a CLD protection strategy in 33 cases of left hemihepatectomy. All patients underwent abdominal MRI before surgery and were informed of the treatment details, including surgical methods, risks, and complications. Finally, the general data of 33 patients, the data on CLD injury, and the change in the volume of the caudate lobe 1 year after the operation were compared with preoperation values. The following method was used to calculate the volume: The sectional area of the caudate lobe is outlined using the imaging system software. The sectional area is multiplied by

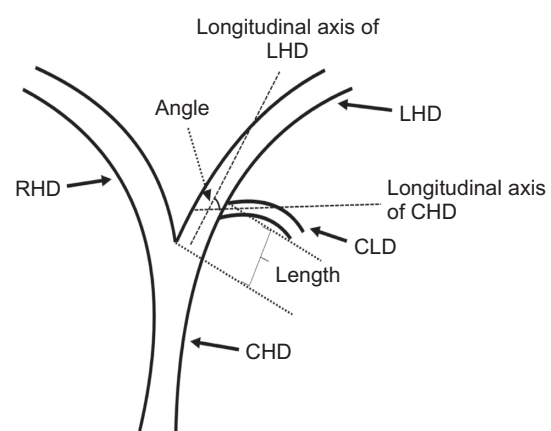


Fig. 1. Schematic diagram for measuring the length and angle of the caudate lobe bile duct (CLD) flowing into the left hepatic duct (LHD). CHD, common hepatic duct; RHD, right hepatic duct.

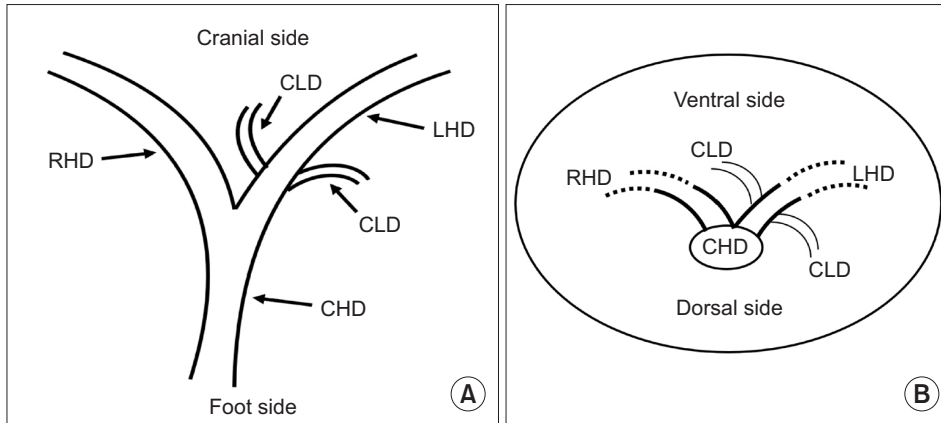


Fig. 2. Schematic diagram of the direction of the caudate lobe bile duct flowing into the left hepatic duct. (A) The coronal plane and (B) the cross-section. CLD, caudate lobe bile duct; LHD, left hepatic duct; RHD, right hepatic duct; CHD, common hepatic duct.

Table 1. Data after length grouping in MRI and T-tube cholangiography

Length (cm)	MRI	T-tube cholangiography
0–0.50	21 (5.3)	3 (3.0)
0.51–1.00	75 (18.8)	15 (15.0)
1.01–1.50	204 (51.0)	61 (61.0)
1.51–2.00	95 (23.8)	19 (19.0)
>2.00	5 (1.3)	2 (2.0)
Total	400 (100)	100 (100)

Values are presented as number (%).

the sectional thickness to obtain the sectional volume, and the volume of the caudate lobe is the sum of the sectional volumes.

Statistical methods

IBM SPSS Statistics ver. 23.0 (IBM Corp.) was used for relevant statistical analysis. Measurement data with a normal distribution are expressed as the mean and standard deviation; counting data are expressed as the frequency (%). In addition, the median (interquartile range) was reported for measurement data with a nonnormal distribution. The Wilcoxon signed rank sum test of paired samples was used for comparisons between groups. A P-value of <0.05 was considered statistically significant.

RESULTS

Imaging results

MRI data from 400 patients and T-tube cholangiography data from 100 patients were successfully collected. The data obtained from the 2 examinations were statistically analyzed. In MRI and T-tube cholangiography, the average length from the confluence point of the CLD into the LHD to the confluence of the left and right hepatic ducts was 1.19 ± 0.40 cm and 1.26 ± 0.39 cm, respectively. The average angle between the longitudinal axis of the CLD entering the LHD and the longitudinal axis of the

Table 2. Data after angle grouping in MRI and T-tube cholangiography

Angle (°)	MRI	T-tube cholangiography
0–45.0	73 (18.3)	15 (15.0)
45.1–90.0	251 (62.8)	70 (70.0)
90.1–135.0	71 (17.8)	13 (13.0)
135.1–180	5 (1.3)	2 (2.0)
Total	400 (100)	100 (100)

Values are presented as number (%).

initial segment of the LHD was $68.27^\circ \pm 22.59^\circ$ and $66.58^\circ \pm 22.88^\circ$, respectively. The patients were divided into 5 groups based on 0.5-cm intervals of duct length. The duct length was 1.01–1.50 cm in 51.0% and 61.0% of the patients based on MRI and T-tube cholangiography data, respectively (Table 1). Patients were divided into 4 groups based on 45° intervals for the measurements of angle between the longitudinal axis of the CLD entering the LHD and the longitudinal axis of the initial segment of the LHD. The angle was 45.1°–90.0 in 62.75% and 70.0% of the patients based on MRI and T-tube cholangiography images, respectively (Table 2). These results indicate that the CLD mostly converged into the LHD at an acute angle. In MRI and T-tube cholangiography, the following directions of the CLD confluence into the LHD were noted: coronal plane mainly (MRI, 79.8%; T-tube, 82.0%), confluence from the foot side to the cranial side, and cross-section mainly with confluence from the dorsal side to the ventral side (MRI, 84.5%; T-tube, 88.0%) (Table 3). Fig. 3 presents the images of data acquisition in MRI and T-tube cholangiography respectively. Supplementary Fig. 1 depicts 8 types of schematic diagrams of the CLD converging into the LHD at acute and obtuse angles on the coronal plane and cross-section. Here, A depicts convergence from the foot side and dorsal side at acute angles; B depicts confluence from the cranial side and dorsal side at acute angle; C depicts confluence from the foot side and dorsal side at an obtuse angle; D depicts confluence from the foot side and ventral side

at an acute angle; E depicts entry from the foot side and ventral side at an obtuse angle; F depicts confluence from the cranial side and ventral side at an acute angle; G depicts entry from the cranial side and dorsal side at an obtuse angle; H depicts entry from the cranial side and ventral side at an obtuse angle. In the MRIs of 400 patients, A–H inflow modes were noted in 54.3%, 15.0%, 13.3%, 9.8%, 2.5%, 2.0%, 2.0%, and 1.3% of patients, respectively.

The CLD protection strategy was adopted in 33 cases of left hemihepatectomy based on imaging rules. All the operations achieved the treatment purpose. After an operation, all patients recovered uneventfully, and no damage to the CLD was noted in any of the operations at present. To determine whether compensatory hyperplasia or atrophy of the caudate lobe occurred postoperatively, we reviewed MRI or CT data 1 year after surgery to compare the volume of the caudate lobe with the preoperative volume. Finally, 2 patients exhibited volume reduction of the caudate lobe (further examination suggested that caudate lobe atrophy was caused by the residue of bile duct stones located in the caudate lobe, which was not due to the CLD injury). Eleven of the remaining 31 patients presented with significant compensatory enlargement of the caudate lobe volume of >30% (Supplementary Fig. 2), and 20 patients had a

slightly enlarged caudate lobe volume that increased by <30% (Table 4). The volume changes before and after surgery were statistically significant ($P < 0.001$) (Table 5). According to the above results for left hemihepatectomy, this protective strategy could achieve effective protection of the CLD.

DISCUSSION

Similar to other liver segments, the caudate lobe has a good blood supply and blood return, and damage to a few blood vessels will not have a considerable impact on liver tissue. The bile duct system is a tree-like structure. If one bile duct is damaged and blocked, its distal branch drainage will also be blocked. Therefore, if the bile duct in the caudate lobe is damaged, the liver tissue in the drainage area will exhibit atrophy or even fibrosis, causing greater damage to the caudate lobe [6]. Protection of the CLD plays an important role in the

Table 3. Data of the confluence directions on the coronal plane and cross-section

Variable	MRI	T-tube cholangiography
Coronal plane		
Cranial side→foot side	81 (20.3)	18 (18.0)
Foot side→cranial side	319 (79.8)	82 (82.0)
Cross-section		
Ventral side→dorsal side	62 (15.5)	12 (12.0)
Dorsal side→ventral side	338 (84.5)	88 (88.0)

Values are presented as number (%).

Table 4. Clinical data of patients

Variable	Data
No. of patients	33
Sex, male:female	18:15
Age (yr)	45.2 ± 13.5
Surgery type, open:laparoscopic	12:21
Type of disease	
Hepatolithiasis	24 (72.7)
Malignant tumor	6 (18.2)
Benign tumor	3 (9.1)
Caudate lobe bile duct injury	0 (0)
Volume of caudate lobe 1 yr after surgery	
Reduction	2 (6.15)
Enlargement <30%	20 (60.6)
Enlargement >30%	11 (33.3)

Values are presented as number only, mean ± standard deviation or number (%).

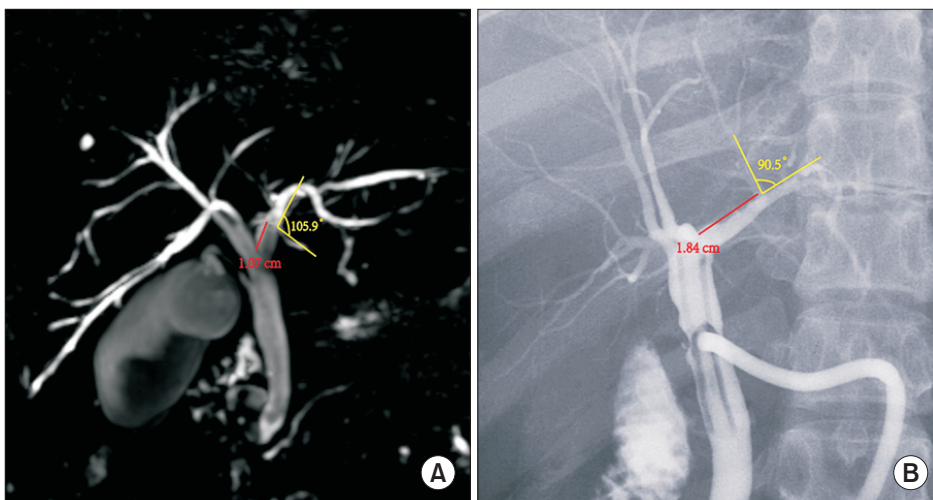


Fig. 3. The images of data acquisition in MRI (A) and T-tube cholangiography (B).

Table 5. The volume changes of the caudate lobe before and after surgery

Variable	Preoperation (n = 33)	Postoperation (n = 33)	Z-value	P-value
Volume of the caudate lobe (cm ³)	15.66 (9.82–22.39)	20.19 (14.32–26.57)	–3.9	<0.001*

Values are presented as median (interquartile range).

*Significant difference.

protection of caudate lobe function. Relevant research on how to transect the LHD to avoid injury to the CLD during left hemihepatectomy is lacking.

The caudate lobe of the liver comprises 3 parts: the left Spiegel lobe, the middle paravena cava, and the right caudate process [7]. Many studies show that most bile ducts in the Spiegel lobe flow into the LHD [8-10]. During left hemihepatectomy, the CLD that flows into the LHD is easily damaged or directly transected in the process of disconnecting the LHD, resulting in a series of complications [11]. However, research on how far away from the confluence and at what angle to transect the LHD is lacking. Different imaging methods such as MRI and T-tube cholangiography, can provide us with information regarding the structure of the hepatobiliary tract, which is of great significance in judging the distance, course, and angle of the CLD flowing into the LHD [12,13]. This study summarized the imaging rule of the CLD confluence into LHD by analyzing MRI images of 400 patients and T-tube angiography images of 100 patients. This rule provides an important basis for the strategy of CLD protection during left hemihepatectomy.

The key to the protection strategy of the CLD is to select a reasonable LHD transection mode. The key point of the transection mode is the length from the junction of the left and right hepatic ducts and the plane of transection. Research shows that the LHD should be transected at the left side of the sagittal part of the portal vein and should not be transected at the root of the LHD so that the complete left CLD opening can be retained. In addition, the left CLD, the right anterior lobe, or the right posterior lobe bile duct with abnormal confluence cannot be transected [14]. However, the above study did not specify the relevant length and plane. We summarized the imaging data and found that most of the CLDs flow into the LHD within 1.5 cm from the junction of the left and right hepatic ducts, and most of the CLDs flow into the LHD at an acute angle from the foot side to the cranial side, and from the dorsal side to the ventral side. However, in clinical practice, most surgeons are accustomed to vertically disconnecting the left hepatic pedicle with an endoscopic gastrointestinal anastomosis stapler after it is separated, which may lead to injury to the confluent bile duct [15]. Compared with the vertical section, the oblique section can make the residual end of the posterior wall of the bile duct slightly longer than the residual end of the anterior wall, so that the posterior wall has a longer separation distance.

In addition, the oblique section allows the operator to better explore whether bile ducts are flowing into the posterior wall after opening the anterior wall of the bile duct.

Therefore, in left hemihepatectomy, the LHD should be transected at least 1.5 cm away from the confluence of the left and right hepatic ducts, and the plane of transection should be oblique to the dorsal side at an angle of 45° with the LHD, which can effectively protect the CLD (Figs. 4, 5). Subsequently, our team adopted this CLD protection strategy in 33 cases of left hemihepatectomy, and the results showed that the CLD and its function were effectively protected without corresponding bile duct injury. A limitation of this study is the lack of complete records on the injury rate of CLDs during surgery in our unit. Thus, a control group for corresponding controlled studies is not available. In the relevant literature, there is a similar lack of statistics about the injury rate of the CLD. However, other studies mentioned that the incidence of bile duct injury was 2.6%–12.0% in open hepatectomy, and this value was higher in laparoscopic surgery [16]. However, there was no injury of the CLD noted in 33 cases in the present study.

The CLD exhibits the same complexity and diversity of anatomical variation as other bile ducts [17]. In cases of CLD anatomical variation or other uncommon confluence modes, such as cranial and ventral, bile duct injury may also occur when employing the transection mode described in this study. Therefore, it is necessary to analyze the rule of the confluence of the CLD in combination with relevant imaging data before surgery and conduct fine anatomy during surgery. If necessary, more information on the confluence of the CLD can be obtained by combining intraoperative ultrasound and indocyanine green fluorescence cholangiography to determine the safe length and plane of disconnection [18]. In cases of corresponding bile duct injury in the caudate lobe, absorbable sutures can be directly used for small ruptures of <3 mm. In addition, T-tube support is recommended for repair of lacerations >3 mm, and the T-tube placement time should be more than 3 months [19,20]. When the continuity of the CLD is interrupted due to transection, it can be repaired by tension-free end-to-end cholangiostomy. The T-tube should be placed at the time of anastomosis, and the placement time is recommended to be at least 6 months [21-23].

In left hemihepatectomy, the LHD should be transected at least 1.5 cm away from the confluence of the left and

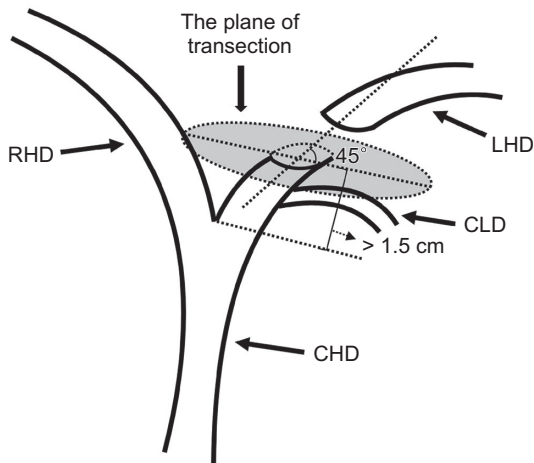


Fig. 4. Schematic diagram of the left hepatic duct transection plane. RHD, right hepatic duct; LHD, left hepatic duct; CLD, caudate lobe bile duct; CHD, common hepatic duct.

right hepatic ducts, and the plane of transection should be oblique to the dorsal side at an angle of 45° with the LHD. Left hemihepatectomy based on these parameters represents an effective strategy to protect the CLD.

SUPPLEMENTARY MATERIALS

Supplementary Figs. 1 and 2 can be found via <https://doi.org/10.4174/astr.2023.105.6.369>.

ACKNOWLEDGEMENTS

The authors would like to thank the imaging center of the Second Affiliated Hospital of Nanchang University for their excellent technical and equipment assistance in data collection and analysis.

Fund/Grant Support

This study was supported by the National Natural Science Foundation of China (82260570).



Fig. 5. One patient's intraoperative bile duct transection plane. Number 1 is a cross-section of the left hepatic duct, and number 2 is a cross-section of the caudate lobe bile duct.

Conflict of Interest

No potential conflict of interest relevant to this article was reported.

ORCID iD

Zhengyi Wu: <https://orcid.org/0000-0002-7096-1988>
 Liang Sun: <https://orcid.org/0000-0002-6069-6279>
 Ke Ning: <https://orcid.org/0000-0002-7588-7801>
 Zhendong Chen: <https://orcid.org/0000-0001-7753-3639>
 Zhipeng Wu: <https://orcid.org/0000-0002-6856-043X>
 Hanqing Yang: <https://orcid.org/0000-0002-9732-0865>
 Jinlong Yan: <https://orcid.org/0000-0001-6234-6224>
 Xiangbao Yin: <https://orcid.org/0009-0007-3398-0040>

Author Contribution

Conceptualization: ZW, JY, XY
 Formal Analysis: ZC, ZW, HY
 Investigation: ZW, LS, KN
 Writing – Original Draft: ZW, LS, KN
 Writing – Review & Editing: JY, XY

REFERENCES

- Sucandy I, Gravetz A, Ross S, Rosemurgy A. Technique of robotic left hepatectomy : how we approach it. *J Robot Surg* 2019;13:201-7.
- Oh HC, Lee SK, Lee TY, Kwon S, Lee SS, Seo DW, et al. Analysis of percutaneous transhepatic cholangioscopy-related complications and the risk factors for those complications. *Endoscopy* 2007;39:731-6.
- Tian J, Li JW, Chen J, Fan YD, Bie P, Wang SG, et al. Laparoscopic hepatectomy with bile duct exploration for the treatment of hepatolithiasis: an experience of 116 cases. *Dig Liver Dis* 2013;45:493-8.
- Dong J, Lau WY, Lu W, Zhang W, Wang J, Ji W. Caudate lobe-sparing subtotal hepatectomy for primary hepatolithiasis.

- Br J Surg 2012;99:1423-8.
5. Aijun L, Jiamei Y, Qinhe T, Mengchao W. Caudate lobe as the sole remnant liver following extended liver resection for hepatocellular carcinoma. *Int J Surg Case Rep* 2014;5:462-4.
 6. Feng X, Dong J. Surgical management for bile duct injury. *Biosci Trends* 2017;11:399-405.
 7. Kumon M, Kumon T, Tsutsui E, Ebashi C, Namikawa T, Ito K, et al. Definition of the caudate lobe of the liver based on portal segmentation. *Glob Health Med* 2020;2:328-36.
 8. Edo H, Sekiguchi R, Edo N, Kajiyama A, Nagamoto M, Gomi T. Evaluation of biliary anatomy in the caudate lobe using drip infusion cholangiography-computed tomography. *Abdom Radiol (NY)* 2019;44:886-93.
 9. Kumon M. Anatomical study of the caudate lobe with special reference to portal venous and biliary branches using corrosion liver casts and clinical application. *Liver Cancer* 2017;6:161-70.
 10. Martins AC, Martins C. Surgical anatomy of caudate bile ducts: silicon-injected cadaveric-livers dissected under magnification. *Ann Hepatobiliary Pancreat Surg* 2020;24:415-20.
 11. Kim JH, Choi JW. Intrahepatic Glissonian approach to the ventral aspect of the Arantius ligament in laparoscopic left hemihepatectomy. *World J Surg* 2019;43:1303-7.
 12. Hyodo T, Kumano S, Kushihata F, Okada M, Hirata M, Tsuda T, et al. CT and MR cholangiography: advantages and pitfalls in perioperative evaluation of biliary tree. *Br J Radiol* 2012;85:887-96.
 13. Umüt T, Remzi E. Correlation among 3-dimensional magnetic resonance cholangiography, intraoperative cholangiography, and intraoperative findings in right liver donors. *Exp Clin Transplant* 2021 Feb 23 [Epub]. <https://doi.org/10.6002/ect.2020.0220>
 14. Birgin E, Reissfelder C, Rahbari NN. Robotic left hepatectomy using the Glissonean pedicle approach for the treatment of Caroli's syndrome. *Zentralbl Chir* 2023;148:129-32.
 15. Yao DB, Wu SD. Application of stapling devices in liver surgery: current status and future prospects. *World J Gastroenterol* 2016;22:7091-8.
 16. Zheng SG. Characteristics and prevention strategies of bile duct injury in laparoscopic hepatectomy. *Chin J Pract Surg* 2018;38:1011-4.
 17. Sugiura T, Nagino M, Kamiya J, Nishio H, Ebata T, Yokoyama Y, et al. Infraportal bile duct of the caudate lobe: a troublesome anatomic variation in right-sided hepatectomy for perihilar cholangiocarcinoma. *Ann Surg* 2007;246:794-8.
 18. Shibata H, Aoki T, Koizumi T, Kusano T, Yamazaki T, Saito K, et al. The efficacy of intraoperative fluorescent imaging using indocyanine green for cholangiography during cholecystectomy and hepatectomy. *Clin Exp Gastroenterol* 2021;14:145-54.
 19. Seeras K, Qasawa RN, Kashyap S, Kalani AD. Bile duct repair [updated 2023 May 22]. In: StatPearls [Internet]. StatPearls Publishing; 2023 Jan-. Available from: <https://www.ncbi.nlm.nih.gov/books/NBK525989/>
 20. Lubikowski J, Piotuch B, Stadnik A, Przedniczek M, Remiszewski P, Milkiewicz P, et al. Difficult iatrogenic bile duct injuries following different types of upper abdominal surgery: report of three cases and review of literature. *BMC Surg* 2019;19:162.
 21. Renz BW, Bösch F, Angele MK. Bile duct injury after cholecystectomy: surgical therapy. *Visc Med* 2017;33:184-90.
 22. Kwak BJ, Choi HJ, You YK, Kim DG, Hong TH. Laparoscopic end-to-end biliary reconstruction with T-tube for transected bile duct injury during laparoscopic cholecystectomy. *Ann Surg Treat Res* 2019;96:319-25.
 23. Ma D, Liu P, Lan J, Chen B, Gu Y, Li Y, et al. A novel end-to-end biliary-to-biliary anastomosis technique for iatrogenic bile duct injury of Strasberg-Bismuth E1-4 treatment: a retrospective study and in vivo assessment. *Front Surg* 2021;8:747304.